A general *in vitro* assay to study enzymatic activities of the ubiquitin system

Boon Keat Chong[1$], Yukun Zuo[1], Kun Jiang, Daniel Finley[2], David Klenerman[1], Yu Ye[1,2#$]

[1]Department of Chemistry, University of Cambridge, Lensfield Road, Cambridge CB2 1EW, United Kingdom

[2]Department of Cell Biology, Harvard Medical School, Longwood Avenue, Boston 02115 MA, United States of America

[$]These authors contributed equally

[#]Email: yy308@cam.ac.uk

Word count: 3679

Abstract

The ubiquitin (Ub) system regulates a wide range of cellular signaling pathways. Several hundred E1, E2 and E3 enzymes are together responsible for the conjugation of Ub to cellular proteins, thereby controlling biological activities. Due to the numerous enzymes and processes involved in ubiquitination, studies on the molecular mechanisms have been challenging. We here report a novel FRET-based assay to study the kinetics of ubiquitination. FRET is established between binding of fluorophore-labeled Ub to eGFP-tagged ZnUBP, a domain that exclusively binds unconjugated Ub. We name this assay the Free Ub Sensor System (FUSS). Using Uba1, UbcH5 and CHIP as model enzymes, we demonstrate that ubiquitination rates can be measured by FUSS using the rate of change in the FRET efficiency over time. Treatment with USP21, a deubiquitinase, removes ubiquitination on CHIP and leads to increased FRET efficiency, confirming the reversibility of the assay. Incubation with tau, a substrate of CHIP, increases the overall ubiquitination activity. We further use this assay to measure the relationship between increasing E1, E2 or E3 concentrations and ubiquitination rates, revealing that Uba1 activity is the rate-limiting step. Our data together demonstrate the versatile applications of a novel ubiquitination assay that does not require labeling of E1, E2, E3 or substrates, and is thus potentially compatible with any E1-E2-E3 combinations. (214 words)

Introduction

Ubiquitination is a posttranslational modification system that dictates the destiny of a wide range of proteins, thereby regulating many key aspects of cell function[1]. The canonical ubiquitination reaction is a multistep process involving E1, E2 and E3 enzymes, which in a sequential manner conjugate free ubiquitin (Ub) to substrates[2]. The E1 enzyme first activates the C-terminus of Ub through ATP hydrolysis and charges the Ub to the active site Cys of E1, resulting in a thioester bond between the enzyme and Ub (E1~Ub)[3]. This activated Ub is then transferred via an E2 and with the help of an E3 enzyme to the substrate, resulting in an isopeptide bond between the C-terminal carboxyl group of Ub and the ε-amino group of a Lys residue of a target protein[4]. A number of deubiquitinases (DUBs) also exist in cells to remove Ub modifications, thereby reversing the ubiquitination process[5].

There are ~40 known E2s, which have an active site Cys that receives the charged Ub moiety from E1 through a thioester transfer reaction. Charged E2~Ub can subsequently either transfer the Ub to the active site Cys of HECT family E3s or directly conjugate Ub to substrates with the help of RING family E3s[6,7]. Typical RING E3s, which represent the majority of the >700 E3s, have no active site Cys and catalyze reactions by bringing together the substrate and the charged E2 in an optimal orientation for conjugation[8]. Two Zn^{2+} ions coordinated by the RING domain is critical for its fold and catalytic activity, though other subfamilies without Zn^{2+}, such as the U-box domain, have been described. The U-box domain is structurally similar to the RING domain, and dimerization is critical for the catalytic activity of both domains.

Ubiquitinated substrates can be modified on either a single residue or multiple residues, known as mono- or multiubiquitination, respectively[9]. The Ub itself may also become ubiquitinated, forming distinct Ub chains (polyubiquitination) on the substrate[10]. The complexity of ubiquitination is further increased by branched or forked Ub chains, where a Ub moiety already part of a chain is further ubiquitinated on a second residue[11]. Moreover, apart from Lys modification, Thr and Ser have also been reported to be ubiquitinated as part of the ERAD[12] or viral infection mechanism[13]. Recently, structural and biochemical studies have characterized a neuron-specific HECT E3 ligase MYCBP2, which specifically ubiquitinates Thr residues on substrates[14]. The ubiquitin system is therefore regulated through layers

of complex enzymatic reactions resulting in a wide range of possible types of Ub modification.

The specificity with which ubiquitination activities regulate cellular functions makes Ub-conjugating and -ligating enzymes as well as DUBs interesting targets of therapeutic intervention[15,16]. A number of experimental assays have been developed to study deubiquitinase activities[17-20]. In comparison, fewer assays are available to measure ubiquitination kinetics of the concerted action of E1, E2 and E3s. Ideally, a general ubiquitination assay should indiscriminately take into account any combination of E1, E2 and E3s that may work together, as well as measure ubiquitination irrespectively of the types of possible ubiquitinated products. Most previous measurements of ubiquitination rates relied on quantification of protein bands from Western blots (e.g.[21-24]). While reliable, SDS-PAGE and antibody detection steps are time-consuming and expensive. Other commercially available kits, such as Lanthascreen[25], depend on the availability and specificity of the antibody against the substrate; or in the case of AMP-Glo[26], uses the ATP hydrolysis rate of E1 to indirectly measure ubiquitination activity, where the activities of E2 and E3 are not directly involved. Currently, no general assay is available to directly measure the concerted activity of ubiquitination irrespective of enzyme combination.

We here report a novel FRET-based assay that enables sensitive measurement of ubiquitination rates in real-time. Changes in the concentration of unconjugated Ub was quantified by the ZnUBP domain of USP5/IsoT. FRET efficiency between fluorophore-labeled Ub and GFP-tagged ZnUBP decreased upon ubiquitination reactions catalyzed by the Uba1-UbcH5-CHIP cascade, while subsequent treatment with the deubiquitinase USP21 restored the FRET signal. Quantification of changes in FRET further enabled calculation of enzyme kinetics. We systematically varied the concentration of E1, E2 or E3 over a wide range and found that changes in the concentration of E1 contributed least to the ubiquitination activity, suggesting the rate-limiting step. Together, we describe a novel ubiquitination assay that directly reports the concerted action of E1-E2-E3 and is optimized for measurements in 96-well plates in a high-throughput manner. As this assay does not require modification or labelling of enzymes involved, it may be applicable to a wide range of Ub-conjugating, deconjugating enzymes and Ub-interacting partners (UbIPs).

Results and Discussion

A novel Free Ub Sensor System (FUSS) to study enzyme kinetics

We expressed and purified recombinant ZnUBP-eGFP fusion protein ($ZnUBP^{eGFP}$) and an N-terminal Cys-modified Ub (Ub^{-1Cys}) construct to apparent homogeneity. Ub^{-1Cys} was subsequently labeled with AlexaFluor-594 (Ub^{594}), which is compatible with eGFP for FRET. We hypothesized that $ZnUBP^{eGFP}$ - Ub^{594} binding would establish FRET, and its efficiency would depend on the concentration of Ub^{594} in solution (**Figure 1a**). Binding of Ub to ZnUBP is well-established and the molecular structure of the protein complex shows that the free C-terminus of Ub, which is buried inside the ZnUBP, is crucial for complex formation[27]. When conjugated, the C-terminus of Ub forms a covalent bond with other proteins and therefore cannot be bound to $ZnUBP^{eGFP}$.

To validate our FRET-based molecular sensor, we titrated Ub^{594} into a cuvette containing $ZnUBP^{eGFP}$ held at a fixed final concentration (0.1 µM, see **Materials and Methods**) and measured the emission spectra from donor excitation (ex_D = 488 nm) in a fluorescence spectrophotometer (**Figure 1b**). Donor eGFP emission (em_D) decreased while the acceptor AF594 emission (em_A) increased with increasing Ub^{594} concentration (**Figure 1c**). The affinity of $ZnUBP^{eGFP}$ - Ub^{594} binding was then quantified from the FRET efficiencies (K_D = 15.6 µM, **Figure 1d**). This K_D value is somewhat higher than previously reported[27] (K_D = 2.8 µM) and may be due to the presence of the bulky eGFP or instrumental differences. Free Ub concentration can therefore be reported by the FRET efficiency according to the relationship established in **Figure 1d**. Our measured binding affinity was confirmed when repeated in a 96-well plate mode and detected by a plate-reader (K_D = 15.7 µM, **SFigure 1**). The optimized assay system, which we will refer to as Free Ub Sensor System (FUSS), consists of 0.1 µM $ZnUBP^{eGFP}$ with Ub^{594} at indicated concentrations.

FUSS detects ubiquitination and deubiquitination events in real-time

We tested whether FUSS is able to report real-time changes in free Ub concentration during a ubiquitination reaction catalyzed by Uba1, UbcH5 and CHIP. The ubiquitination scheme (**Figure 2a**) involving these three enzymes has been characterized before[28-30] and involves Ub-charging and ATP hydrolysis by

Uba1[31] (step 1) followed by Ub-charging of UbcH5[32] (step 2). Charged UbcH5 (UbcH5~Ub) is able to modify other Ub moieties, resulting in free Ub chains[33] (step 5). Alternatively, UbcH5~Ub may bind to dimerized and catalytic active CHIP[34] (step 3), which readily ubiquitinates itself through a mechanism that is not fully understood[28]. Repeated ubiquitination of CHIP by UbcH5~Ub ultimately results in CHIP-polyUb (step 4). As CHIP-polyUb accumulates, the concentration of free Ub will decrease leading to more Ub dissociating from ZnUBP (decreased FRET efficiency). Lastly, Ub moieties on CHIP-polyUb can be removed by DUBs (step 6), regenerating free Ub that can again associate with ZnUBP (increased FRET efficiency). Although it is possible for Uba1~Ub, UbcH5~Ub or CHIP~Ub to discharge into free Ub and enzymes without their subsequent steps leading to ubiquitination, the rates of such reaction are negligible and not considered here[35].

The emission spectra (ex_{488}) for this ubiquitination reaction were measured over time after adding ATP to the FUSS assay (Ub^{594} = 80 µM) containing Uba1, UbcH5 and CHIP (0.5 µM each, **Figure 2b**, *top*). As expected for reduced free Ub concentration, em_D increased while em_A decreased over time (**Figure 2b**, *middle*), and the resulting change in FRET fitted to a single-exponential decay function (**Figure 2b**, *bottom*).

To further confirm that FUSS is a reversible system, USP21 (10 nM final concentration) was added to the same cuvette after 2.5 hrs and emission spectra were collected (**Figure 2c**, *top*). USP21 is a promiscuous and highly active enzyme that deubiquitinates conjugated Ub moieties in an indiscriminate manner[36,37]. Interestingly, em_A increased and reached plateau faster than in **Figure 2b**, while the decrease in em_D was relatively moderate (**Figure 2c**, *middle*). The change in FRET efficiency over time also obeyed a single-exponential function (**Figure 2c**, *bottom*) with a steeper initial gradient compared to the ubiquitination reaction. In both **Figure 2b** and **c** the FRET efficiency versus time plots (*bottom*) were more similar to em_A than em_D versus time plots (*middle*), suggesting that em_A dominates the behavior of FRET efficiency. To quantify the initial rates of reaction in terms of Ub^{594} concentration, we used the binding curve established in **Figure 1d** to convert the FRET efficiency value to Ub concentration (see *equation 4*, **Materials and Methods**), from which the gradient was calculated. The results indicated a faster recovery (initial rate ~8.8 nM s^{-1}) following USP21 treatment compared to ubiquitination (~2.4 nM s^{-1}). Both the ubiquitination and deubiquitination activities

were validated by fluorescence scans of Ub^{594} bands on reaction products separated by SDS-PAGE as well as on Western blots against CHIP (**Figure 2d**).

Replacing AlexFluor-594 with AlexaFluor-647 on Ub did not affect detection of ubiquitination events measured in cuvettes, further validating the robustness of our system (**SFigure 2a** and **b**). Ub^{647} showed however less efficient FRET in the plate-reader and was therefore not used further for measurement (see relevant sections below). To investigate the role of CHIP in the ubiquitination reaction, we repeated the reaction with only Uba1 and UbcH5 in the cuvette containing the FUSS assay and found that a detectable decrease in FRET efficiency could only be measured at a very high UbcH5 concentration (**SFigure 2c**). The relatively small decrease in FRET is likely due to formation of diUb chains, which was confirmed by fluorescence scanning of the reaction products separated by SDS-PAGE (**SFigure 2d**). We further confirmed that only when CHIP was included with Uba1 and UbcH5 did polyubiquitination occur (**SFigure 2e**). These results together suggest that CHIP serves as the substrate that becomes polyubiquitinated and that this is the main reaction detected by FUSS.

Enzyme kinetics of ubiquitination determined by FUSS

The sensitivity of FUSS was tested by gradually lowering Ub^{594} concentration in the cuvettes. At $[Ub^{594}]$ = 35 µM, the em_A, em_D and FRET efficiency versus time plots no longer followed single-exponential functions (**Figure 3a**) and the initial rates were calculated from the gradient of a linear fit of initial time points. The linear relationship of change in FRET efficiency over time is even more apparent at $[Ub^{594}]$ = 2 µM, where em_D remained unchanged while em_A dominated the appearance of the FRET plot (**Figure 3b**). Insensitivity of em_D to Ub^{594} at lower initial concentrations is likely due to the smaller fraction of bound $ZnUBP^{eGFP}$. Additionally, with decreasing Ub^{594} concentration a lag phase became more apparent (~3 min in **Figure 3b**) before the major decrease in FRET efficiency. This has been observed in previous assays but not described as part of the ubiquitination assay and not taken into account in rate calculations[38]. Possibly, Ub charging by E1 requires binding to both Ub and ATP, which would require ATP hydrolysis and then a second Ub adenylation step before E1~Ub can be formed[39]. Since ATP is in excess (10 mM), this step would be limited by the Ub concentration.

We subsequently determined the initial rates at various Ub^{594} concentrations and plotted an "apparent Michaelis-Menten" curve to characterize the relationship between reaction rates and Ub concentration (**Figure 3c**). The apparent $K_{50\%}$ (19.1 ± 6.5 µM) represents the concentration of Ub^{594} at which the reaction rate is half of V_{max} (2.9 ± 0.3 nM s^{-1}), and conceptually equivalent to Michaelis constant (K_M). K_M is only valid when describing a scenario where Uba1, UbcH5 and CHIP would form a stable enzymatic complex, which is not applicable here. The values we determined for $K_{50\%}$ and V_{max} were useful in comparing between cuvette-based and plate-reader measurements (see below).

FUSS is suitable for high-throughput ubiquitination assays

Although sensitive, measurements on fluorescence spectrophotometers require substantial sample volume (50 µl per cuvette) and are limited by the number of cuvettes as well as the time it takes to scan the entire emission spectrum. To enable enzymatic measurements in a high-throughput manner that would be applicable to screening of large compound libraries, we repeated the FUSS assays in **Figure 3** in a 96-well plate measured on a fluorescence monochromator plate-reader, which comfortably detected a reaction volume of 20 µl. FRET efficiency decreased after ATP was added to the sample, confirming the sensitivity of FUSS on the plate-reader (**Figure 4a**, *top*). Although the loss in FRET efficiency is evident compared to the same reaction mixture measured without ATP (**Figure 4a**, *bottom*) the magnitude of FRET change is smaller than expected from cuvette-based measurements.

We suspected photo-bleaching of the eGFP[40] due to the higher laser power required for sensitivity on the plate-reader. Our suspicion was confirmed when we studied the em_D and em_A signals from the reactions with or without ATP (**Figure 4b**, *top* and *bottom*, respectively). Since the majority of $ZnUBP^{eGFP}$ is bound by Ub^{594} in the absence of ATP in the reaction, the donor eGFP is able to transfer fluorescence energy to the Ub^{594} acceptor and thus remain photostable. Such phenomena have been reported and experimentally validated by several previous studies (e.g. [41]). We could therefore observe decreasing em_D only in the catalyzed and not the uncatalyzed ubiquitination reaction. Adding ATPγS, an analog of ATP, showed the same result as with the uncatalyzed reaction (data not shown).

To verify this photo-bleaching effect, we added CHIP-polyUb^{594} products generated from a FUSS reaction in **Figure 3** to a 96-well plate and measured the FRET efficiency following USP21 treatment. As expected, em_A decreased while em_D did not increase as significantly as in **Figure 3**, suggesting photo-bleaching of the donor eGFP while free Ub^{594} released could bind ZnUBP^{eGFP} (**Figure 4c**).

Given that eGFP photo-bleached rapidly upon Ub^{594} dissociation, we calculated the FRET efficiencies using em_D values from Ub^{594}-associated ZnUBP^{eGFP}. Since the same final concentration of ZnUBP^{eGFP} (0.1 µM) was used in all FUSS reactions, we repeatedly measured ZnUBP^{eGFP} bound to 5 µM Ub^{594} and calculated an average em_D (standard deviation < 15%, n = 6) versus time plot (**SFigure 3a**). The em_D did not change in the presence of Ub^{594} and remained stable over time, comparable to the em_D behavior measured in cuvettes (**SFigure 3b**). This average em_D was substituted into FRET efficiency calculations together with the measured em_A, to compare between reactions performed on the plate-reader.

We subsequently used FUSS to measure em_A ubiquitination reactions of Uba1-UbcH5-CHIP (each at 0.5 µM final concentration) at increasing Ub^{594} concentrations and determined the calculated FRET curves, which were sensitive to changes in Ub concentration on the nanomolar scale (**SFigure 4a**). The initial rates of reaction were extrapolated from each curve (*equation 5*, **Materials and Methods**), plotted against Ub concentration and fitted with the Michaelis-Menten equation as described above, from which the apparent $K_{50\%}$ (76.9 ± 61.2 µM) and V_{max} (4.7 ± 2.2 nM s^{-1}) were determined (**Figure 4d**). These values are comparable to those determined from cuvette-based measurements in **Figure 3**, confirming the validity of our approach. Towards the end of reaction, samples were analyzed by Western blot to confirm the increase in the level of ubiquitinated CHIP at higher Ub concentrations (**Figure 4e**). The ubiquitination pattern is in agreement with Ub bands detected by fluorescence scans in protein gels (**SFigure 4b**).

E1 activity is rate-limiting in the ubiquitination reaction

The rate of ubiquitination depends not only on Ub concentration but also the concentrations of Uba1, UbcH5 and CHIP. We therefore investigated the relationship between enzyme concentration and ubiquitination rate in 96-well plates in a high-throughput manner. Each well contained the FUSS ([Ub^{594}] = 5 µM) with E1, E2 or E3 at increasing concentrations whilst the concentration of the other two enzymes

remained unchanged (0.5 μM each). Starting off with CHIP, we measured and calculated the initial rates of reaction as described earlier, which revealed a sigmoidal relationship with CHIP concentration and reached a maximum rate when [CHIP] > 2 μM (**Figure 5a**). This appeared to be concurrent with a changing pattern of CHIP ubiquitination from high molecular weight (MW) smears to distinct ubiquitinated CHIP bands between 40-100kDa (**Figure 5b** and **SFigure 5a**). Excluding the highest CHIP concentration data point, which no longer obeyed the sigmoidal relationship, permitted data extrapolation using the Hill equation (Hill coefficient = 1.5 ± 0.6, K_{half} of 0.81 ± 0.3 μM).

The correlation between ubiquitination rates and UbcH5 concentrations could also be described using the Hill equation (Hill coefficient = 1.1 ± 0.6, K_{half} of 0.26 ± 0.1 μM, **Figure 5b**). The maximum rate of ubiquitination reached a plateau at 1.1 ± 0.1 nM s^{-1} ([UbcH5] = 5 μM), consistent with the maximum rate described in **Figure 5a** (plateau value 0.9 ± 0.1 nM s^{-1}). As with CHIP, very high UbcH5 concentrations did not appear to support further increase in ubiquitination rate. Western blot of reaction samples also showed a reduction in the level of CHIP-polyUb (**Figure 5d** and **SFigure 5b**) at high UbcH5 concentrations, validating the observations in **Figure 5c**.

In comparison, no clear relationship was detected between Uba1 concentration and ubiquitination rates (**Figure 5e**) and the maximum rate at 0.5 ± 0.06 nM s^{-1} (when [Uba1] = 2 μM) was much lower than those found for CHIP and UbCH5. This indicates that ubiquitination rate cannot reach the same level as with CHIP and UbcH5 regardless of the increase in Uba1 concentration, suggesting that Uba1-catalysed activities are the rate-limiting step in this ubiquitination pathway. In fact, CHIP-polyUb level decreased at very high Uba1 concentrations (**Figure 5f** and **SFigure 5c**), suggesting a slower rate of ubiquitination.

Possibly, the reduced ubiquitination rates at high enzyme concentrations could be due to competition between charged and uncharged enzymes for the same binding sites, so that the Ub-charged enzyme cannot transfer its Ub moiety down the E1-E2-E3 pathway for ubiquitination. For instance, at high concentrations most of UbcH5 will remain uncharged ([UbcH5] > [Ub] = 5 μM), but still able to bind CHIP[42] and potentially limiting the likelihood of UbcH5~Ub interacting with CHIP. The rate therefore reduces as [UbcH5] increases beyond 5 μM. An additional source of the reduced ubiquitination rate could be due to futile cycles of Ub-charging and

discharging without Ub transfer to the enzyme downstream, reportedly influenced by the level of enzymes present[35]. The rates determined by FUSS reflect the overall ubiquitination activity irrespective of individual processes, and investigations into the detailed events of each enzyme would be too complex for our assay.

Our FUSS assay is optimized to measure the overall ubiquitination activity, making it less sensitive for detecting the distinct types of products formed. This is seen when smears of polyubiquitinated CHIP appear to shift to low MW bands with increasing E2 or E3 concentration, indicating lesser extent of Ub-modification per CHIP molecule (**Figure 5a** and **b**). A second example is the assembly of free Ub chains at low UbcH5 concentrations, which when increased appears to shift towards ubiquitination of CHIP (**SFigure 5b**). Perhaps, as the concentration of UbcH5 increases the level of free Ub would decrease, making CHIP the more likely recipient of Ub from UbcH5~Ub. We are cautious in comparing initial rates measured by FUSS with these Western blots and proteins gels, which reflect products formed towards the end of reactions. Specific labeling of UbcH5 or CHIP would be required to measure the formation of each of these products using FUSS.

Rate of ubiquitination increases in the presence of tau

Under physiological conditions CHIP ubiquitinates misfolded proteins and aggregates and target these for degradation[29,43]. One substrate of CHIP is tau[44-46], an amyloidogenic protein that is often associated with Alzheimer's disease[47]. We assessed whether the presence of a true substrate would alter the overall ubiquitination rate in FUSS reactions containing Uba1, UbcH5 and CHIP (0.5 µM each) as well as tau (10 µM final concentration). Higher initial rates of ubiquitination were observed in the presence of tau (e.g. 1.5 nM ± s^{-1} at [Ub^{594}] = 20 µM, **Figure 6a**) compared to those at the same Ub^{594} concentrations but in the absence of tau (0.8 nM ± s^{-1} at [Ub^{594}] = 20 µM). Ubiquitination on tau was confirmed by Western blot (**Figure 6b**), and the level of CHIP-polyUb remained largely the same between reactions in presence or absence of tau (**Figure 6c**). Together, these results suggest that the overall rate of ubiquitination does increase in presence of tau, and CHIP readily modifies both itself and its natural substrate.

The results presented in this study demonstrate that FUSS is a robust assay sensitive to changes in the concentration of free Ub in solution. Such change could be due to

the activity of any enzyme or combination of enzymes with the ability to conjugate or deconjugate Ub. Depending on the requirement of individual studies, our system may be further modified to e.g. introduce modifications on the Ub moiety to prevent discharging from E2 or E3s (e.g. [48,49]), thus enabling investigations of distinct ubiquitination steps (see **Figure 2a**). A second feasible application would be to measure binding affinity of UbIPs (Ub-interacting partners) using FUSS, which will show reduced fluorescence as the UbIP is titrated into the solution[20]. Finally, wild-type Ub (Ub^{WT}) could be mixed with and used to compete with Ub^{594} for binding with $ZnUBP^{eGFP}$, reducing the FRET signal. In line with this idea, the FUSS could further be engineered so that the binding of Ub^{594} would be weaker than Ub^{WT} and at the same time unable to be charged by E1. Any ubiquitination will then result in binding of Ub^{594} to $ZnUBP^{eGFP}$ previously occupied by Ub^{WT}, increasing the FRET signal. This approach would be especially useful in measuring ubiquitination or deubiquitination activity in cell lysates. Together, our FUSS assay offers a simple proof-of-principle approach to study the enzymes of the ubiquitin system and enable the wider scientific community interested in the ubiquitin system to study its enzymes.

Acknowledgement

YY conceptualized research idea, prepared reagents, performed experiments, analyzed the data and wrote the manuscript. KJ purified proteins and performed experiments. YZ provided kinetic analysis of enzymatic reactions. BKC measured enzymatic reactions under supervision of YY. DF and DK provided reagents. This project was funded by a Sir Henry Wellcome Fellowship awarded to YY.

Figure Legends

Figure 1. Establishing the free ubiquitin sensor system (FUSS). **(a)** A molecular model (pdb-id 2G45) of FUSS, where the Ub (yellow) is labeled at its N-terminus with a AlexaFluor-594 dye (red) and the ZnUBP domain (forest) is fused at its C-terminus with an eGFP (green). Specific binding between the Ub C-terminus (ball-and-stick) to the ZnUBP site is shown (*right*), enabling FRET from eGFP to the dye. **(b)** Emission spectra (500-750 nm) collected using fluorescence excitation at 488 nm. Ub^{594} was titrated at the color-coded final concentrations into a cuvette containing $ZnUBP^{eGFP}$, continuously kept at 0.1 µM final concentration. A representative set of data from three repeats (n=3) is shown. **(c)** Donor (green) and acceptor (scarlet) fluorescence calculated from integrated areas in **b** between 500-560 nm and 610-670 nm, respectively. **(d)** Mean FRET efficiencies calculated from the donor and emission fluorescence intensities performed in triplicate (n=3). Error bars from standard deviations in all cases were smaller than the size of the data points. The binding constant is extrapolated from fitting the data to the equation for single-site binding (*equation 3*, **Materials and Methods**).

Figure 2. Measuring protein ubiquitination with FUSS. **(a)** A schematic representation of the major ubiquitination processes measured by FUSS. A proportion of the free Ub^{594} pool (scarlet) is bound by $ZnUBP^{eGFP}$ (green) in a concentration-dependent manner (see **Figure 1**). In the presence of ATP, Uba1 (E1) charges free Ub^{594}, forming Uba1~Ub (*step 1*). This Ub is then transferred from Uba1 to the active site of UbcH5 (E2), leading to UbcH5~Ub formation (*step 2*). UbcH5~Ub may either transfer the charged Ub to a second Ub to synthesize Ub chains (*step 5*) or to the active site of CHIP (E3) in *step 3*. Charged CHIP is then able to ubiquitinate itself and ultimately result in CHIP-polyUb. Dimerization of CHIP is required for this activity, though the details of this reaction are not fully understood. Ubiquitination on CHIP can be removed by USP21 (DUB), regenerating free Ub moieties and unmodified CHIP (*step 6*). **(b)** A ubiquitination reaction was set up in a cuvette containing Uba1, UbcH5 and CHIP (0.5 µM final concentration each) mixed with FUSS ([Ub] = 80 µM final concentration). Emission spectra before (green) and after adding ATP (various shades of red) were collected continuously (*top*). Arrows indicate the direction of peak change over time. For clarity, 5 min intervals between spectra are presented after

reaction initiation. Change in donor (green) and acceptor (scarlet) fluorescence intensity over time were then calculated from the spectra (*middle*). Calculated FRET efficiency change over time fitted with a single-exponential decay function (*bottom*). **(c)** The completed reaction from **b** was treated with USP21 (10 nM final concentration). Emission spectra before (green) and after (red) adding USP21 are shown (*top*). Donor and acceptor spectra (*middle*) and the calculated FRET efficiencies (*bottom*) over time are shown as in **b**. Data have been fitted to a single-exponential decay function where possible. All experiments presented have been repeated three times (n = 3). **(d)** Completed reactions from **b** and **c** were quenched with LDS buffer containing reducing agents, separated by SDS-PAGE and detected by fluorescence scanning against Ub^{594} (*left*) or Western blot staining against CHIP using secondary antibodies labeled with AlexaFluor 647 (*right*).

Figure 3. The apparent Michaelis-Menten ubiquitination reaction measured by the spectrophotometer. **(a)** Donor (green) and acceptor (scarlet) fluorescence intensities (*left*) and calculated FRET efficiencies (*right*) measured after ATP addition. The reaction was prepared in a cuvette as in **Figure 2**, [Ub] = 35 µM. Single-exponential decay function (dotted line) does not fit the data and the initial rate was calculated from the gradient of the linear fit (blue solid line) of the earlier of data points. **(b)** FUSS measurement performed and presented as in **a**, [Ub] = 2 µM. **(c)** Initial rates of reaction measured at various Ub concentrations (calculated using *equation 4* in **Materials and Methods**) fitted to the Michaelis-Menten equation (*equation 7*) to extrapolate apparent values of $K_{50\%}$ and V_{max}. Error bars represent the standard error of the mean for three independent measurements (n=3).

Figure 4. FUSS is compatible with plate-reader assays for the measurement of ubiquitination reactions. **(a)** Calculated FRET efficiency over time in a FUSS reaction ([Ub^{594}] = 20 µM) containing Uba1, UbcH5 and CHIP (each at 0.5 µM) measured on a 96-well plate (*top*). The same setup is measured without adding ATP (*bottom*). **(b)** Donor (green) and acceptor (scarlet) intensities over time used for FRET calculation in **a**. **(c)** Detection of deubiquitinase activity in 96-well plate mode. A reaction containing CHIP-polyUb (ubiquitinated with 65 µM Ub^{594}) was mixed with 10 nM USP21. The donor and acceptor intensities (*top*) and the calculated FRET (*bottom*) are shown. **(d)** Initial rates of reaction extracted from **SFigure 4** (calculated using

equation 5 in **Materials and Methods**) were fitted to the Michaelis-Menten equation (*equation 7*). Error bars represent the standard error of the mean for three repeat measurements (n=3). **(e)** Anti-CHIP Western blot of the reactions in **d** quenched with LDS buffer containing reducing agent. The various forms of CHIP are indicated. The secondary antibody was labeled with AlexaFluor-647 and the blot was detected using a Typhoon fluorescence scanner (see **Materials and Methods**). Numbers to the left represent molecular weight markers.

Figure 5. Systematic assessment of the relationship between enzyme concentration and ubiquitination rates. **(a)** CHIP at increasing concentrations was incubated with FUSS reactions ([Ub^{594}] = 5 µM) containing Uba1 and UbcH5 at 5 µM each. The initial rates of reaction are shown in a semi-log plot against CHIP concentration and fitted with the Hill equation (excluding 50 µM). **(b)** Western blot against CHIP of the reactions in **a** after 150 min. A sample of uncatalyzed reaction (lane 1) and a sample of Ub^{594} only (lane 11) were included as controls. All samples were quenched with LDS buffer containing reducing agent. **(c)** UbcH5 at increasing concentrations was incubated with FUSS reactions ([Ub^{594}] = 5 µM) containing Uba1 and CHIP at 5 µM each. The initial rates of reaction were fitted with the Hill equation (excluding 50 µM) as in **a**. **(d)** Anti-CHIP Western blot of the reactions in **c** after 150 min, performed as in **b**. **(e)** Uba1 at increasing concentrations was incubated with FUSS reactions ([Ub^{594}] = 5 µM) containing UbcH5 and CHIP at 5 µM each. **(f)** Anti-CHIP Western blot of the reactions in **e** after 150 min. Error bars represent the standard error of the mean for three repeat measurements (n=3).

Figure 6. Adding tau increases the rate of ubiquitination. **(a)** Uba1, UbcH5 and CHIP (5 µM each) with or without 10 µM tau was mixed with FUSS reactions ([Ub^{594}] at 2, 5, 10 or 20 µM) and the initial rates of reaction plotted against Ub^{594} concentration. **(b)** Anti-tau Western blot of samples in **a** with tau (lanes 1-4) and without tau (lanes 5-8) run next to each other. A sample of tau only (lane 11) is included as a control. **(c)** Fluorescence scan against Ub^{594} of the samples in **b** separated by SDS-PAGE. A sample of Ub594 only (lane 1) is included as a control. All samples were quenched with LDS buffer containing reducing agent before separation on SDS-PAGE.

SFigure 1. The relationship between FRET and Ub concentration measured on a plate-reader. Mean FRET efficiencies were calculated from the measured donor and emission fluorescence intensities performed in triplicate (n=3). Error bars representing standard deviations in all cases were smaller than the size of data points. The binding constant is extrapolated from fitting the data to the equation for single-site binding (*equation 3*, **Material and Methods**).

SFigure 2. Polyubiquitination bands represent modification on CHIP. **(a)** FUSS reaction was set up in a cuvette with Ub^{647} at 0.5 µM and Uba1, UbcH5 and CHIP (0.5 µM final concentration each). Measurements were performed as in **Figure 2**, with 5 min interval time between measurements. **(b)** Calculated FRET efficiencies from the data in **a**. **(c)** Ubiquitination reaction containing Uba1 at 0.5 µM and Ub^{647} at 5 µM required high UbcH5 concentration (40 µM) for FUSS to detect a change in FRET efficiency. **(d)** Product of the reaction in **c** separated by SDS-PAGE and scanned on typhoon detects free Ub chains. **(e)** Ubiquitination reactions containing FUSS (Ub^{647} at 5 µM) mixed with Uba1 only (lane 1), Uba1 with UbcH5 (lane 2) or Uba1, UbcH5 and CHIP at high- (lane 3) or low concentrations (lane 5). The ubiquitinated products in lane 5 are deubiquitinated by USP21 (lane 4). All reactions were incubated for 2 hrs and quenched with LDS buffer with reducing agent before separation by SDS-PAGE, followed by visualization on a Typhoon scanner.

SFigure 3. Donor fluorescence does not suffer from photo-bleaching when bound to Ub^{594}. **(a)** Mean values of six independent measurements of $ZnUBP^{eGFP}$ (0.1 µM) bound to 5 µM Ub^{594} and measured over time on the plate-reader. Error bars represent standard deviation from the mean (n=6). **(b)** FUSS assay ($[Ub^{594}]$ = 5 µM) set up as in **Figure 3** to acquire donor and acceptor emissions (*left*) and the calculated FRET (*right*). The donor fluorescence does not change at this concentration of Ub^{594} even as ubiquitination reaction continues.

SFigure 4. Plate-reader measurements of ubiquitination reactions at increasing Ub concentrations. **(a)** Calculated FRET efficiencies using the measured emission intensity over time and the donor fluorescence in **SFigure 3a**. Ub^{594} concentrations (2, 5, 10, 20, 40 and 80 µM) used in FUSS assays are indicated on each plot. Representative data of three repeat measurements (n=3) are shown here. **(b)** The

reactions in **a** were quenched with LDS buffer and fresh reducing reagent after completion, separated by SDS-PAGE and scanned on a typhoon scanner to detect ubiquitinated bands.

SFigure 5. Ubiquitination pattern changes with enzyme concentration. Separation on SDS-PAGE of completed reactions from **(a)** CHIP concentration gradient in **Figure 5a**, **(b)** UbcH5 concentration gradient in **Figure 5b,** and **(c)** Uba1 concentration gradient in **Figure 5c**, scanned on Typhoon to detect ubiquitinated bands. The final concentrations of each protein are indicated on the top of every lane. All samples were quenched with LDS buffer containing fresh reducing agent.

Materials and Methods

Molecular Biology

ZnUBP domain (encoding residues 174-289 of human USP5/IsoT) was cloned into a pOPINGFP vector resulting in the DNA sequence of eGFP fused in frame to the 3'-end of ZnUBP (kindly shared by David Komander). The ubiquitin construct in pOPINS vector was modified at 5'-end to include codons for Cys and Ala before the start of the first Met[20]. The resulting construct translated into a fusion protein His_6-SUMO-Cys-Ala-ubiquitin. Plasmids for full-length mouse CHIP in pGEX-6P vector (kind gift from Sophie Jackson), full-length mouse Uba1 in pET28a, human UbcH5a in pGEX-6P and human USP21[36] in pOPINS vector were used for protein expression (kind gifts from David Komander).

Protein purification

Plasmids were transformed into BL21 cells and grown at 37 °C shaking conditions in LB media until O.D. >1.0. At this cell density cultures were induced with 1 mM IPTG and incubated overnight at 20 °C. Subsequently, cells were collected by centrifugation at 4800 rpm using a JLA-8.1000 rotor on an Avanti J-26 XP (Beckman, Palo Alto, USA). Cell pellets were resuspended in 40 ml of Lysis buffer (200 mM NaCl, 10 mM DTT, 25 mM Tris, pH 8.0) for GST-tagged proteins, or Buffer A (300 mM NaCl, 10 mM imidazole, 50 mM Tris, pH 7.4) for His_6-tagged proteins. Cell lysis was achieved by sonication and the lysate was cleared by centrifugation at 20,000 rpm for 30 min using a pre-chilled JA-25.50 rotor at 4 °C on Avanti J-26 XP.

For affinity purification of GST-tagged proteins, the cleared cell lysate filtered through a 0.45 μm filter and incubated with 2-3 ml glutathione beads in a glass column for 1 hr under constant agitation at 4 °C. Subsequently, the beads were washed with 1 l of High salt buffer (500 mM NaCl, 5 mM DTT, 25 mM Tris, pH 8.5) and 1 l of Low salt buffer (50 mM NaCl, 5 mM DTT, 25 mM Tris, pH 8.5) to remove non-specific proteins. PreScission protease was then added to the beads in Low salt buffer and incubated overnight at 4 °C. On the next day, the protein of interest was eluted from the beads. Eluted fractions that were more than 90% pure on Coomassie-stained protein gels were pooled and concentrated to >1 mg/ml and flash-frozen.

For affinity purification of His6-tagged proteins, the cleared cell lysate was filtered through a 0.22 μm filter and loaded onto a pre-packed TALON column pre-

charged with cobalt ions. Unbound proteins were washed out with 50 ml of Buffer A and the protein of interest was eluted using Buffer A + 200 mM imidazole (pH adjusted to 7.4). The eluted protein fractions were pooled and dialyzed against Low salt buffer overnight at 4 °C. Proteins expressed from pOPINS vectors were incubated with SENP1 protease during the dialysis to remove the N-terminal His_6-SUMO tag.

USP21 and Ub^{-1Cys} were further purified by pre-packed Resource-S and Mono-S (GE Healthcare) cation-exchange chromatography columns, respectively, with a linear salt gradient reaching 0.5 M NaCl. $ZnUBP^{eGFP}$ was loaded onto Resource-Q anion-exchange column running the same linear gradient. All three proteins eluted very early from the column and fractions containing the protein of interest were concentrated to 2-5 ml and loaded onto a Superdex75 gel-filtration column in Protein buffer (50 mM NaCl, 50 mM Tris, 1 mM DTT, pH 7.4). Fractions from the major peak containing the protein of interest were pooled together, concentrated and assessed on SDS-PAGE to be pure before being flash-frozen at >1 mg/ml concentration. All column chromatography methods were performed at 4 °C on an AKTA Purifier system.

Full-length tau (isoform 0N4R) was purified as described before[50].

Protein labeling

AlexaFluor-594 C5 maleimide and AlexaFluor-647 C2 maleimide were dissolved in DMSO (10 mM final concentration), flash-frozen in 20 µl aliquots and stored at -80 °C. Labeling of Ub^{-1Cys} was achieved by reacting ~300 µM of Ub in Labeling buffer (1 mM TCEP, 50 mM Tris, pH 7.2) with 1.2-fold molar excess of dye. The reaction mixture was agitated in the dark at room temperature for three hours. Unreacted dye was removed by size-exclusion chromatography (HiLoad S26/10 column). Labeled proteins were concentrated to > 200 µM concentration as measured on nanodrop.

FUSS and ubiquitination reactions

$ZnUBP^{eGFP}$ and Ub^{594} were diluted in Protein buffer down to the desired concentration. The final concentration of $ZnUBP^{eGFP}$ was 0.1 µM in all the reactions. Stock $ZnUBP^{eGFP}$ and Ub^{594} were kept on ice while setting up the reaction mixtures, which were then allowed 5 min to equilibrate before measurement. For cuvette-based titration experiments in **Figure 1**, Ub^{594} was serially diluted in Protein buffer

containing $ZnUBP^{eGFP}$ at 0.1 µM so as to keep the final $ZnUBP^{eGFP}$ concentration constant.

Protein ubiquitination reactions were performed in Protein buffer. $ZnUBP^{eGFP}$ and Ub^{594} were mixed with Uba1, UbcH5 and CHIP and incubated for 5 min to allow equilibration. The reaction volume for cuvette-based experiments was 50 µl and 20 µl per well in a 96-well plate. Ubiquitination reactions were initiated by adding stock 250 mM ATP.$MgCl_2$ (pH-adjusted to 7.0) to a final concentration of 10 mM in the reaction.

Fluorescence measurements

Cary Eclipse spectrophotometer (Varian Inc.) was used for cuvette-based fluorescence measurements. The fluorescent sample was loaded in a quartz cuvette (Hellma) with 3.0 x 10.0 mm windows placed so that detection would be perpendicular to the excitation light path. For fluorescence emission scans the excitation maximum wavelength was set to 488 nm with ± 5 nm window. PMT charge was set (700 V) so that the emission maximum lies approximately half-way between the minimum and maximum fluorescence detection limits. Donor and acceptor intensities were calculated from the integral of the spectrum between 500 to 560 nm and 610 to 670 nm, respectively. The interval time between measurements was set to 1 min unless otherwise indicated.

Clariostar plate-reader (BMG Labtech) was used for fluorescence measurements of multiple reactions simultaneously. Each reaction contained 20 µl of sample volume in black 96-well round-bottom plates (Corning Life Sciences). The focal height was adjusted to the fluorescence intensity of the most concentrated sample. Each well was excited with 10 flash pulses and measured for 200 cycles with 60 s per cycle under 'plate mode'. The fluorescence gain for the donor (ex_{440-10}) and the acceptor (em_{610-10}) was set to 2000, unless otherwise indicated. The wells were covered with a sealable aluminum foil and a small amount of water was added between the wells to reduce evaporation during data recording.

Fluorescence scans of protein gels and Western blots

Reaction samples were taken and quenched with LDS buffer and reducing agent (Invitrogen) in a 2:1 volumetric ratio (sample:LDS). Proteins were separated on NuPAGE Bolt 4-12% SDS-polyacrylamide gels (Invitrogen) and subsequently

scanned on a Typhoon scanner using the indicated excitation (633 nm) and emission (670 nm) module to detect Ub^{594} bands. Alternatively, a Trans-blot (Biorad) system was used to transfer proteins separated by SDS-PAGE to PVDF membranes. Primary rabbit monoclonal anti-CHIP (EPR4447, Abcam) or mouse monoclonal anti-tau (1E1/A6, Millipore) were recognized by secondary anti-rabbit or anti-mouse antibodies carrying AlexaFluor-647 labels (Invitrogen) and detected on the Typhoon scanner using the same module as above.

Data analysis

All data analyses were carried out on Prism 6 (GraphPad) unless otherwise indicated.

FRET efficiency values reported in this manuscript are calculated using the equation:

$$FRET = \frac{em_A}{em_D + em_A} \qquad (1)$$

where em_D and em_A are emission intensities of the donor and acceptor, respectively.

The binding constant, K_D, describes the relationship between bound and unbound $ZnUBP^{eGFP}$ and is defined by the equation below:

$$K_D = \frac{[ZnUBP^{eGFP}] \times [Ub^{594}]}{[ZnUBP^{eGFP} - Ub^{594}]} \qquad (2)$$

where $[ZnUBP^{eGFP}]$ and $[Ub^{594}]$ are the concentrations of the free protein and ligand, respectively, and $[ZnUBP^{eGFP} - Ub^{594}]$ that of the bound complex.

Experimentally, the binding constant is derived from data extrapolation by applying the following equation:

$$FRET = \frac{[Ub^{594}] \times FRET_{max}}{[Ub^{594}] + K_D} \qquad (3)$$

Cuvette-based FRET measurements are converted to Ub^{594} concentrations using the function from **Figure 1d**:

$$[Ub^{594}] = \frac{15.6 \times FRET}{1.056 - FRET} \quad (4)$$

and that from **SFigure 1** to convert plate-reader based FRET:

$$[Ub^{594}] = \frac{15.7 \times FRET}{0.75 - FRET} \quad (5)$$

where the Ub^{594} concentration is in µM.

Initial rates of reaction are calculated from linear fits to the first 10 min (or the first 10 data points) after the measured start of the reaction using the equation below:

$$[Ub^{594}] = m \times time + constant \quad (6)$$

where m is the gradient representing the initial rate.

Plots in **Figure 3c** and **Figure 4d** are fitted to the Michaelis-Menten equation:

$$v_0 = \frac{V_{max} \times [Ub^{594}]}{K_M + [Ub^{594}]} \quad (7)$$

where v_0 is the initial rate of reaction.

Plots in **Figure 5** are fitted to the Hill equation:

$$v_0 = \frac{V_{max} \times [Ub^{594}]^h}{K_{half}{}^h + [Ub^{594}]^h} \quad (8)$$

where K_{half} is the enzyme concentration at half-maximal value of V_{max} and h is the Hill coefficient.

References

1. Oh E, Akopian D, Rape M (2018) Principles of Ubiquitin-Dependent Signaling. *Annu Rev Cell Dev Biol* **34**: 137–162.
2. Komander D, Rape M (2012) The ubiquitin code. *Annu Rev Biochem* **81**: 203–229.
3. Schulman BA, Harper JW (2009) Ubiquitin-like protein activation by E1 enzymes: the apex for downstream signalling pathways. *Nat Rev Mol Cell Biol* **10**: 319–331.
4. Hershko A, Ciechanover A (1998) The ubiquitin system. *Annu Rev Biochem* **67**: 425–479.
5. Mevissen TET, Komander D (2017) Mechanisms of Deubiquitinase Specificity and Regulation. *Annu Rev Biochem*.
6. Stewart MD, Ritterhoff T, Klevit RE, Brzovic PS (2016) E2 enzymes: more than just middle men. *Cell Res* **26**: 423–440.
7. Ye Y, Rape M (2009) Building ubiquitin chains: E2 enzymes at work. *Nat Rev Mol Cell Biol* **10**: 755–764.
8. Deshaies RJ, Joazeiro CAP (2009) RING Domain E3 Ubiquitin Ligases. *Annu Rev Biochem* **78**: 399–434.
9. Kulathu Y, Komander D (2012) Atypical ubiquitylation - the unexplored world of polyubiquitin beyond Lys48 and Lys63 linkages. *Nature Publishing Group* **13**: 508–523.
10. Swatek KN, Komander D (2016) Ubiquitin modifications. *Nature Publishing Group* **26**: 399–422.
11. Meyer H-J, Rape M (2014) Enhanced Protein Degradation by Branched Ubiquitin Chains. *Cell* **157**: 910–921.
12. Shimizu Y, Okuda-Shimizu Y, Hendershot LM (2010) Ubiquitylation of an ERAD substrate occurs on multiple types of amino acids. *Molecular Cell* **40**: 917–926.
13. Wang X, Herr RA, Chua WJ, Lybarger L, Wiertz EJHJ, Hansen TH (2007) Ubiquitination of serine, threonine, or lysine residues on the cytoplasmic tail can induce ERAD of MHC-I by viral E3 ligase mK3. *The Journal of Cell Biology* **177**: 613–624.
14. Pao K-C, Wood NT, Knebel A, Rafie K, Stanley M, Mabbitt PD, Sundaramoorthy R, Hofmann K, van Aalten DMF, Virdee S (2018) Activity-based E3 ligase profiling uncovers an E3 ligase with esterification activity. *Nature* **556**: 381–385.
15. Huang X, Dixit VM (2016) Drugging the undruggables: exploring the ubiquitin system for drug development. *Nature Publishing Group* **26**: 484–498.
16. Nalepa G, Rolfe M, Harper JW (2006) Drug discovery in the ubiquitin–proteasome system. *Nat Rev Drug Discov* **5**: 596–613.
17. Hospenthal MK, Mevissen TET, Komander D (2015) Deubiquitinase-based analysis of ubiquitin chain architecture using Ubiquitin Chain Restriction (UbiCRest). *Nat Protoc* **10**: 349–361.
18. Geurink PP, van Tol BDM, van Dalen D, Brundel PJG, Mevissen TET, Pruneda JN, Elliott PR, van Tilburg GBA, Komander D, Ovaa H (2016) Development of Diubiquitin-Based FRET Probes To Quantify Ubiquitin Linkage Specificity of Deubiquitinating Enzymes. *Chem Eur J of Chem Bio* **17**: 816–820.

19. Virdee S, Ye Y, Nguyen DP, Komander D, Chin JW (2010) Engineered diubiquitin synthesis reveals Lys29-isopeptide specificity of an OTU deubiquitinase. *Nature Chemical Biology* **6**: 750–757.
20. Ye Y, Blaser G, Horrocks MH, Ruedas-Rama MJ, Ibrahim S, Zhukov AA, Orte A, Klenerman D, Jackson SE, Komander D (2012) Ubiquitin chain conformation regulates recognition and activity of interacting proteins. *Nature* **492**: 266–270.
21. Saha A, Lewis S, Kleiger G, Kuhlman B, Deshaies RJ (2011) Essential Role for Ubiquitin-Ubiquitin-Conjugating Enzyme Interaction in Ubiquitin Discharge from Cdc34 to Substrate. *Molecular Cell* **42**: 75–83.
22. Petroski MD, Deshaies RJ (2005) In Vitro Reconstitution of SCF Substrate Ubiquitination with Purified Proteins. In, *High Level Expression and Purification of Recombinant SCF Ubiquitin Ligases* pp 143–158. Elsevier.
23. Keszei AFA, Sicheri F (2017) Mechanism of catalysis, E2 recognition, and autoinhibition for the IpaH family of bacterial E3 ubiquitin ligases. *Proceedings of the National Academy of Sciences* **114**: 1311–1316.
24. Kovacev J, Wu K, Spratt DE, Chong RA, Lee C, Nayak J, Shaw GS, Pan ZQ (2014) A SnapShot of Ubiquitin Chain Elongation. *Journal of Biological Chemistry* **289**: 7068–7081.
25. Carlson CB, Horton RA, Vogel KW (2009) A Toolbox Approach to High-Throughput TR-FRET-Based SUMOylation and DeSUMOylation Assays. *ASSAY and Drug Development Technologies* 090616052833001–090616052833008.
26. Mondal S, Hsiao K, biochemistry SGA, 2016 (2016) A bioluminescent assay for monitoring conjugation of ubiquitin and ubiquitin-like proteins. *Analytical Biochemistry* **510**: 41–51.
27. Reyes-Turcu FE, Horton JR, Mullally JE, Heroux A, Cheng X, Wilkinson KD (2006) The Ubiquitin Binding Domain ZnF UBP Recognizes the C-Terminal Diglycine Motif of Unanchored Ubiquitin. *Cell* **124**: 1197–1208.
28. Nikolay R, Wiederkehr T, Rist W, Kramer G, Mayer MP, Bukau B (2004) Dimerization of the Human E3 Ligase CHIP via a Coiled-coil Domain Is Essential for Its Activity. *Journal of Biological Chemistry* **279**: 2673–2678.
29. Murata S, Minami Y, Minami M, Chiba T, Tanaka K (2001) CHIP is a chaperone-dependent E3 ligase that ubiquitylates unfolded protein. *EMBO reports* **2**: 1133–1138.
30. Page RC, Pruneda JN, Amick J, Klevit RE, Misra S (2012) Structural insights into the conformation and oligomerization of E2~ubiquitin conjugates. *Biochemistry* **51**: 4175–4187.
31. Haas AL, Rose IA (1982) The mechanism of ubiquitin activating enzyme. A kinetic and equilibrium analysis. *Journal of Biological Chemistry* **257**: 10329–10337.
32. Olsen SK, Capili AD, Lu X, Tan DS, Lima CD (2010) Active site remodelling accompanies thioester bond formation in the SUMO E1. *Nature* **463**: 906–912.
33. Buetow L, Gabrielsen M, Anthony NG, Dou H, Patel A, Aitkenhead H, Sibbet GJ, Smith BO, Huang DT (2015) Activation of a primed RING E3-E2-ubiquitin complex by non-covalent ubiquitin. *Molecular Cell* **58**: 297–310.
34. Soss SE, Yue Y, Dhe-Paganon S, Chazin WJ (2011) E2 conjugating enzyme selectivity and requirements for function of the E3 ubiquitin ligase CHIP. *J Biol Chem* **286**: 21277–21286.

35. Özkan E, Yu H, Deisenhofer J (2005) Mechanistic insight into the allosteric activation of a ubiquitin-conjugating enzyme by RING-type ubiquitin ligases. *Proc Natl Acad Sci USA* **102**: 18890–18895.
36. Ye Y, Akutsu M, Reyes-Turcu F, Enchev RI, Wilkinson KD, Komander D (2011) Polyubiquitin binding and cross-reactivity in the USP domain deubiquitinase USP21. *EMBO reports* **12**: 350–357.
37. Faesen AC, Luna-Vargas MPA, Geurink PP, Clerici M, Merkx R, van Dijk WJ, Hameed DS, Oualid El F, Ovaa H, Sixma TK (2011) The differential modulation of USP activity by internal regulatory domains, interactors and eight ubiquitin chain types. *Chem Biol* **18**: 1550–1561.
38. Krist DT, Park S, Boneh GH, Rice SE, Statsyuk AV (2016) UbFluor: a mechanism-based probe for HECT E3 ligases. *Chemical Science* **7**: 5587–5595.
39. Olsen SK, Lima CD (2013) Structure of a Ubiquitin E1-E2 Complex: Insights to E1-E2 Thioester Transfer. *Molecular Cell* **49**: 884–896.
40. Cranfill PJ, Sell BR, Baird MA, Allen JR, Lavagnino Z, de Gruiter HM, Kremers G-J, Davidson MW, Ustione A, Piston DW (2016) Quantitative assessment of fluorescent proteins. *Nature Methods* **13**: 557–562.
41. Basu S, Needham L-M, Lando D, Taylor EJR, Wohlfahrt KJ, Shah D, Boucher W, Tan YL, Bates LE, Tkachenko O, et al. (2018) FRET-enhanced photostability allows improved single-molecule tracking of proteins and protein complexes in live mammalian cells. *Nat Commun* **9**: 2520.
42. Xu Z, Kohli E, Devlin KI, Bold M, Nix JC, Misra S (2008) Interactions between the quality control ubiquitin ligase CHIP and ubiquitin conjugating enzymes. *BMC Struct Biol* **8**: 26.
43. Tawo R, Pokrzywa W, Kevei É, Akyuz ME, Balaji V, Adrian S, Höhfeld J, Hoppe T (2017) The Ubiquitin Ligase CHIP Integrates Proteostasis and Aging by Regulation of Insulin Receptor Turnover. *Cell* **169**: 470–482.e13.
44. Dickey CA, Yue M, Lin W-L, Dickson DW, Dunmore JH, Lee WC, Zehr C, West G, Cao S, Clark AMK, et al. (2006) Deletion of the Ubiquitin Ligase CHIP Leads to the Accumulation, But Not the Aggregation, of Both Endogenous Phospho- and Caspase-3-Cleaved Tau Species. *The Journal of* ….
45. Petrucelli L (2004) CHIP and Hsp70 regulate tau ubiquitination, degradation and aggregation. *Human Molecular Genetics* **13**: 703–714.
46. Shimura H, Schlossmacher MG, Hattori N, Frosch MP, Trockenbacher A, Schneider R, Mizuno Y, Kosik KS, Selkoe DJ (2001) Ubiquitination of a new form of alpha-synuclein by parkin from human brain: implications for Parkinson's disease. *Science* **293**: 263–269.
47. Goedert M, Eisenberg DS, Crowther RA (2017) Propagation of Tau Aggregates and Neurodegeneration. *Annu Rev Neurosci* **40**: 189–210.
48. Wickliffe KE, Lorenz S, Wemmer DE, Kuriyan J, Rape M (2011) The Mechanism of Linkage-Specific Ubiquitin Chain Elongation by a Single-Subunit E2. *Cell* **144**: 769–781.
49. Cui J, Yao Q, Li S, Ding X, Lu Q, Mao H, Liu L, Zheng N, Chen S, Shao F (2010) Glutamine deamidation and dysfunction of ubiquitin/NEDD8 induced by a bacterial effector family. *Science* **329**: 1215–1218.
50. Cliffe R, Sang JC, Kundel F, Finley D, Klenerman D, Ye Y (2019) Filamentous Aggregates Are Fragmented by the Proteasome Holoenzyme. *Cell Reports* **26**: 2140–2149.e2143.

Figure 1

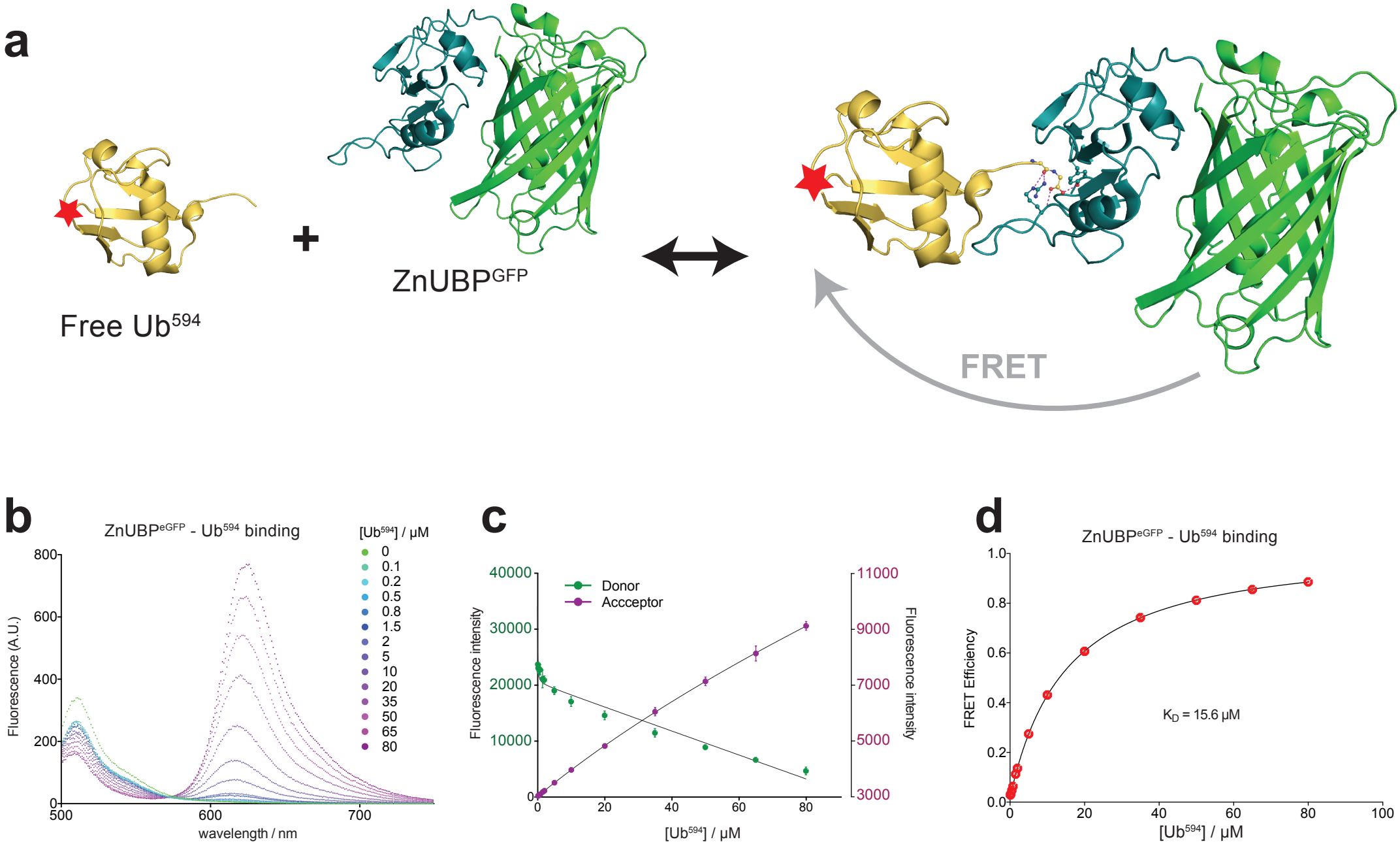
a
Free Ub594
+
ZnUBPGFP
FRET
b
ZnUBPeGFP - Ub594 binding
[Ub594] / µM
0
0.1
0.2
0.5
0.8
1.5
2
5
10
20
35
50
65
80
Fluorescence (A.U.)
wavelength / nm
c
Donor
Accceptor
Fluorescence intensity
[Ub594] / µM
d
ZnUBPeGFP - Ub594 binding
FRET Efficiency
KD = 15.6 µM
[Ub594] / µM

Figure 2

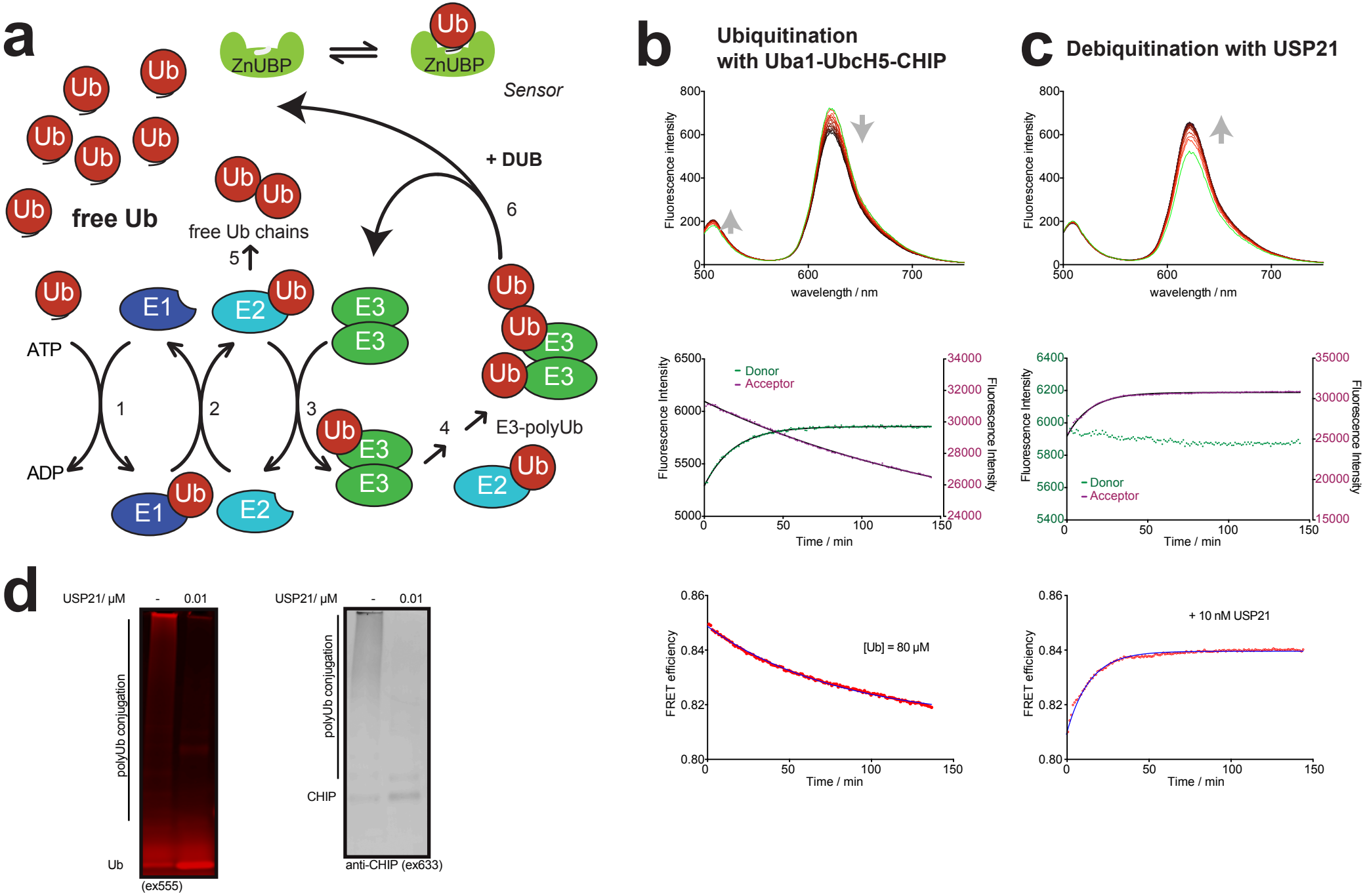
a
ZnUBP
Ub
ZnUBP
Sensor
+ DUB
free Ub
free Ub chains
ATP
ADP
E1
E2
E3
E3-polyUb
1
2
3
4
5
6
b
Ubiquitination with Uba1-UbcH5-CHIP
Fluorescence intensity
wavelength / nm
Donor
Acceptor
Fluorescence Intensity
Time / min
FRET efficiency
[Ub] = 80 μM
c
Debiquitination with USP21
+ 10 nM USP21
d
USP21/ μM
-
0.01
polyUb conjugation
Ub
(ex555)
CHIP
anti-CHIP (ex633)

Figure 3

a

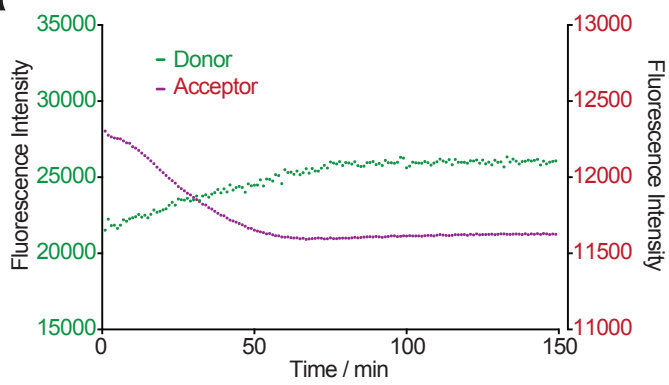
Donor
Acceptor
Fluorescence Intensity
Fluorescence Intensity
Time / min
35000
30000
25000
20000
15000
13000
12500
12000
11500
11000
0
50
100
150

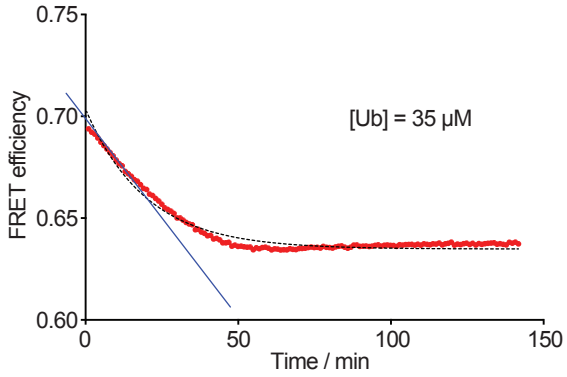
[Ub] = 35 μM
FRET efficiency
Time / min
0.75
0.70
0.65
0.60
0
50
100
150

b

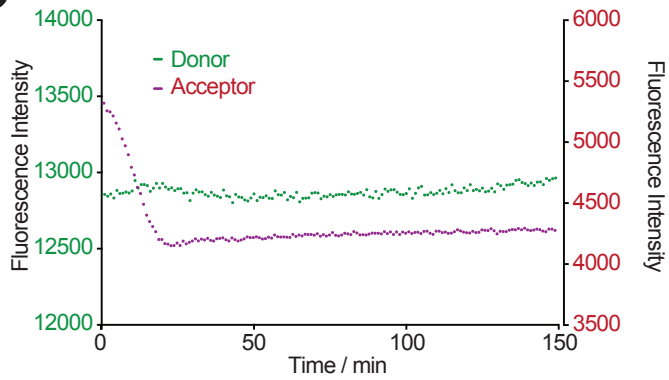
Donor
Acceptor
Fluorescence Intensity
Fluorescence Intensity
Time / min
14000
13500
13000
12500
12000
6000
5500
5000
4500
4000
3500
0
50
100
150

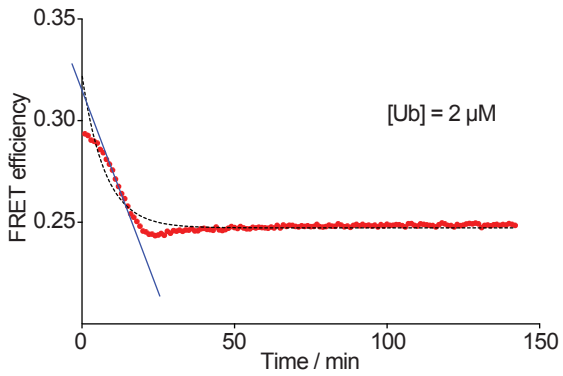
[Ub] = 2 μM
FRET efficiency
Time / min
0.35
0.30
0.25
0
50
100
150

c

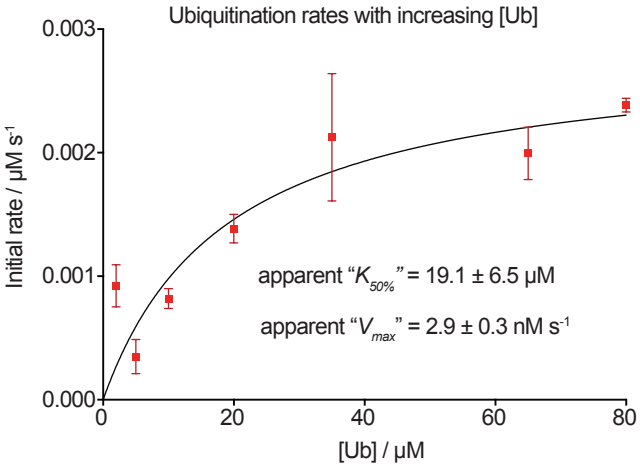
Ubiquitination rates with increasing [Ub]
Initial rate / μM s-1
[Ub] / μM
0.003
0.002
0.001
0.000
0
20
40
60
80
apparent "K50%" = 19.1 ± 6.5 μM
apparent "Vmax" = 2.9 ± 0.3 nM s-1

Figure 4

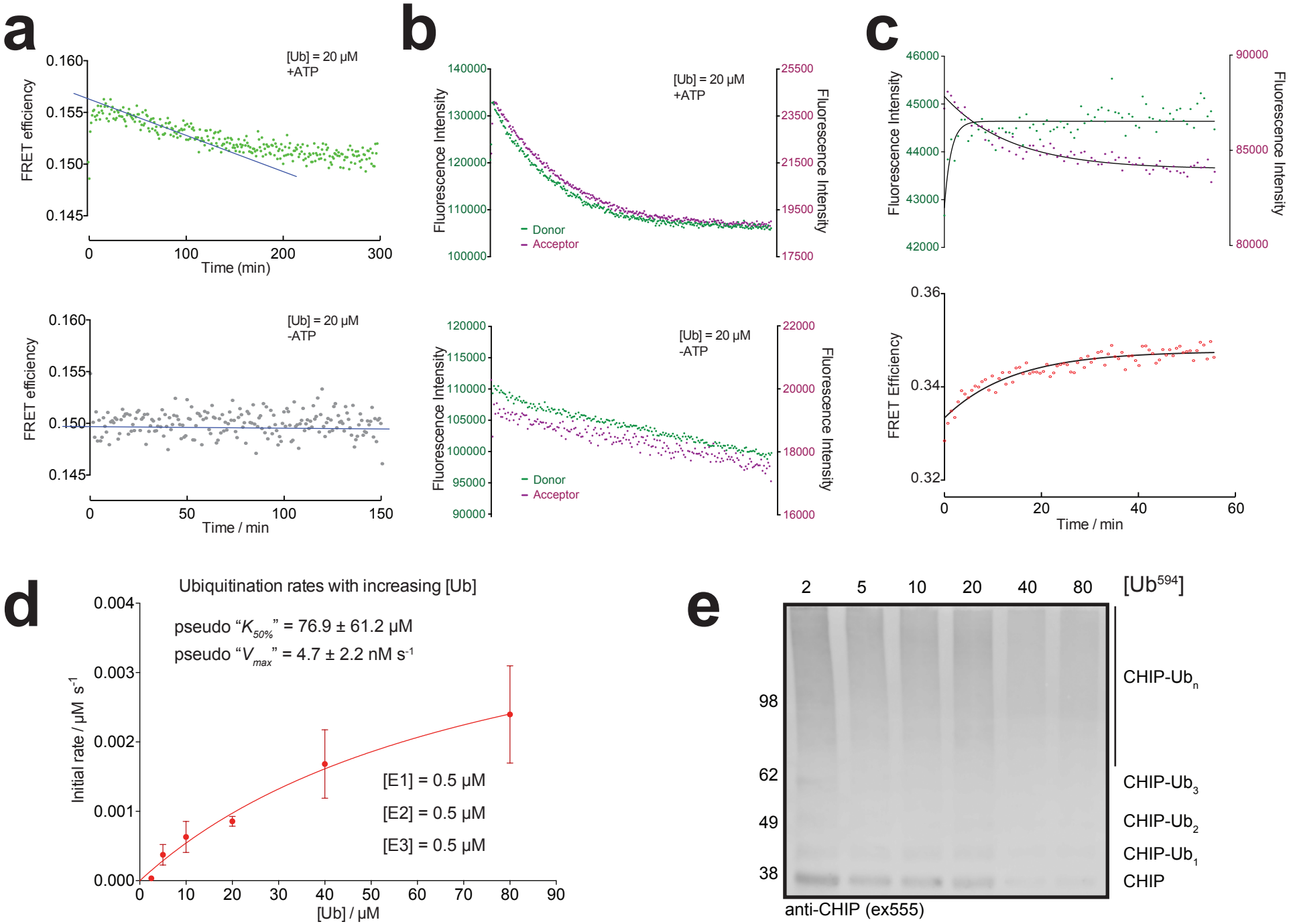
a
[Ub] = 20 μM
+ATP
FRET efficiency
0.160
0.155
0.150
0.145
0
100
200
300
Time (min)
[Ub] = 20 μM
-ATP
FRET efficiency
0.160
0.155
0.150
0.145
0
50
100
150
Time / min
b
[Ub] = 20 μM
+ATP
Fluorescence Intensity
140000
130000
120000
110000
100000
25500
23500
21500
19500
17500
Donor
Acceptor
[Ub] = 20 μM
-ATP
Fluorescence Intensity
120000
115000
110000
105000
100000
95000
90000
22000
20000
18000
16000
Donor
Acceptor
c
Fluorescence Intensity
46000
45000
44000
43000
42000
90000
85000
80000
FRET Efficiency
0.36
0.34
0.32
0
20
40
60
Time / min
d
Ubiquitination rates with increasing [Ub]
pseudo "$K_{50\%}$" = 76.9 ± 61.2 μM
pseudo "V_{max}" = 4.7 ± 2.2 nM s^{-1}
Initial rate / μM s^{-1}
0.004
0.003
0.002
0.001
0.000
[E1] = 0.5 μM
[E2] = 0.5 μM
[E3] = 0.5 μM
0
10
20
30
40
50
60
70
80
90
[Ub] / μM
e
2
5
10
20
40
80
[Ub^{594}]
98
62
49
38
CHIP-Ub_n
CHIP-Ub_3
CHIP-Ub_2
CHIP-Ub_1
CHIP
anti-CHIP (ex555)

Figure 5

a

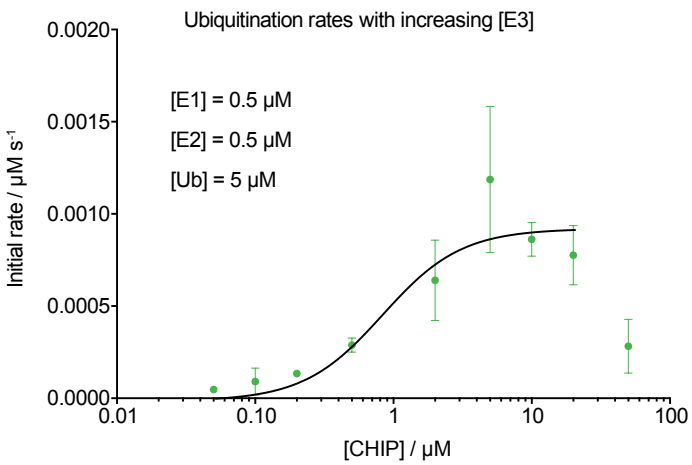

c

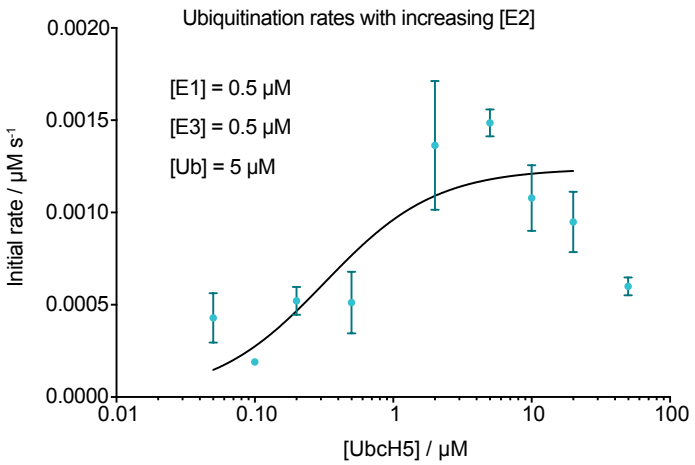

e

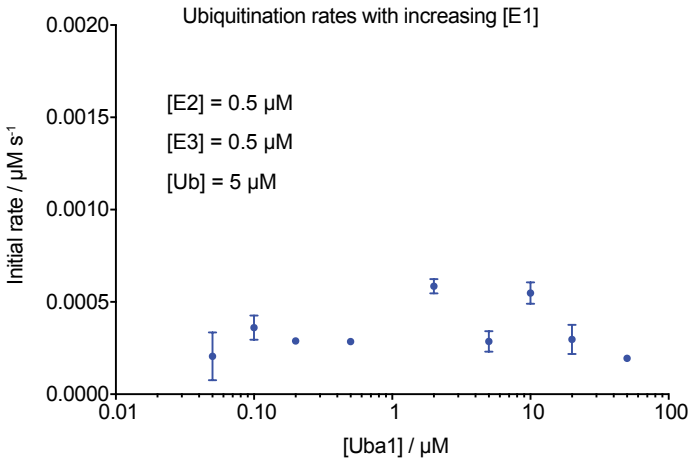

b

Uba1 / μM	0.5	0.5	0.5	0.5	0.5	0.5	0.5	0.5	0.5	0.5	0
UbcH5 / μM	0.5	0.5	0.5	0.5	0.5	0.5	0.5	0.5	0.5	0.5	0
CHIP / μM	**0.05**	**0.05**	**0.1**	**0.2**	**0.5**	**2**	**5**	**10**	**20**	**50**	**0**
[Ub^{594}] / μM	5	5	5	5	5	5	5	5	5	5	5
ATP	-	+	+	+	+	+	+	+	+	+	+

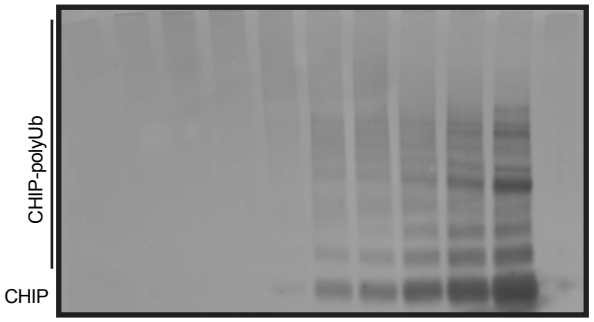

anti-CHIP (ex555)

d

Uba1 / μM	0.5	0.5	0.5	0.5	0.5	0.5	0.5	0.5	0.5	0.5	0
UbcH5 / μM	**0.5**	**0.05**	**0.1**	**0.2**	**0.5**	**2**	**5**	**10**	**20**	**50**	**0**
CHIP / μM	0.5	0.5	0.5	0.5	0.5	0.5	0.5	0.5	0.5	0.5	0
[Ub^{594}] / μM	5	5	5	5	5	5	5	5	5	5	5
ATP	-	+	+	+	+	+	+	+	+	+	+

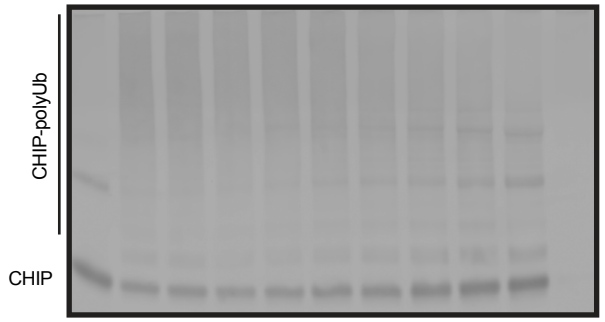

anti-CHIP (ex555)

f

Uba1 / μM	**0.05**	**0.1**	**0.2**	**0.5**	**2**	**5**	**10**	**20**	**50**	**0.5**	**0**
UbcH5 / μM	0.5	0.5	0.5	0.5	0.5	0.5	0.5	0.5	0.5	0.5	0
CHIP / μM	0.5	0.5	0.5	0.5	0.5	0.5	0.5	0.5	0.5	0.5	0
[Ub^{594}] / μM	5	5	5	5	5	5	5	5	5	5	5
ATP	+	+	+	+	+	+	+	+	+	-	+

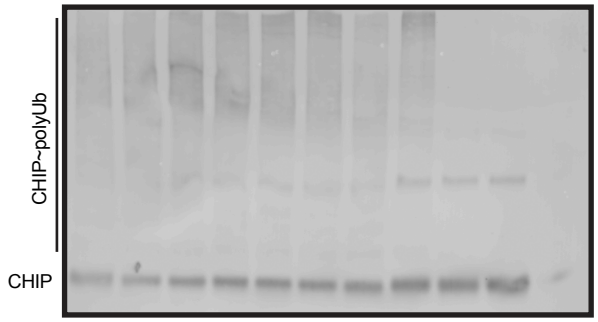

anti-CHIP (ex555)

Figure 6

a

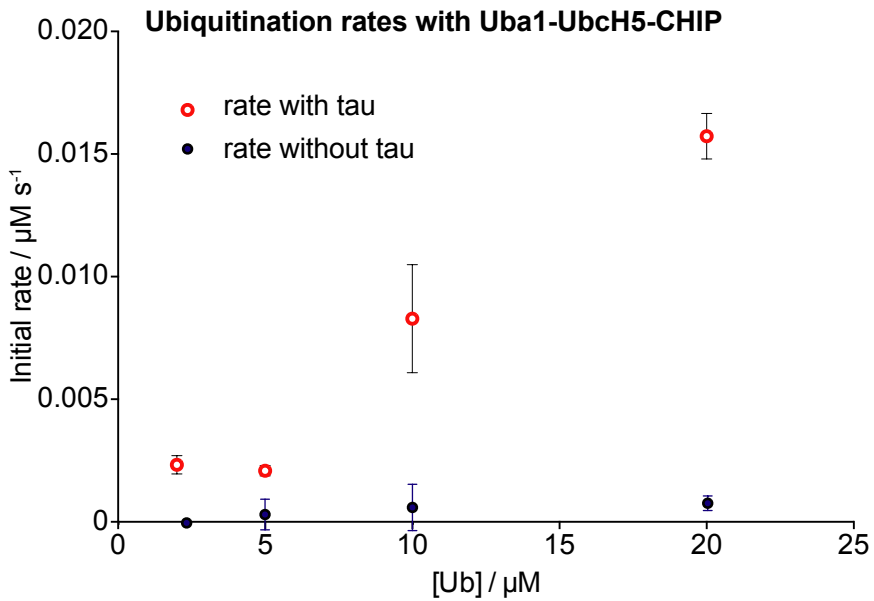

b

Uba1	+	+	+	+	+	+	+	+	-	-
UbcH5	+	+	+	+	+	+	+	+	-	-
CHIP	+	+	+	+	+	+	+	+	-	-
tau	+	+	+	+	-	-	-	-	-	+
[Ub^{594}]	2	5	10	20	2	5	10	20	5	0

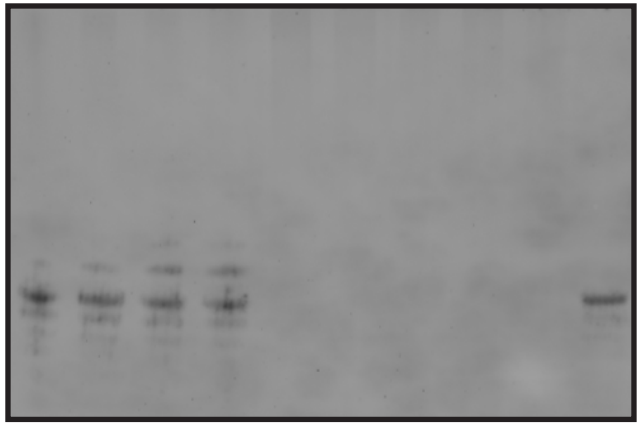

anti-tau (ex647)

c

Uba1	-	+	+	+	+	+	+	+	+
UbcH5	-	+	+	+	+	+	+	+	+
CHIP	-	+	+	+	+	+	+	+	+
tau	-	+	+	+	+	-	-	-	-
[Ub^{594}]	10	2	5	10	20	2	5	10	20

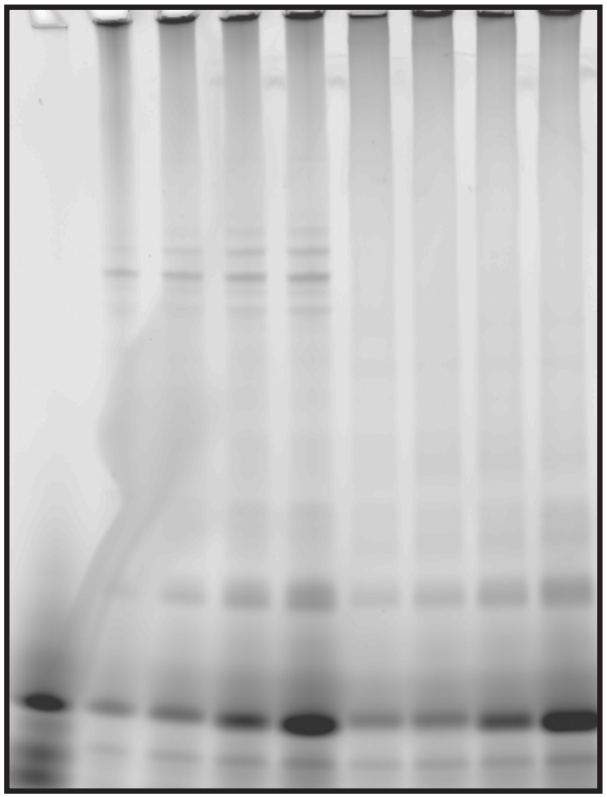

(ex555)